

Inferring the structural properties of eddies in the log layer from spectral statistics

Lionel Agostini and Michael Leschziner

Aeronautics Department
Imperial College London
Prince Consort Rd. London SW7 2AZ
l.agostini@imperial.ac.uk and mike.leschziner@imperial.ac.uk

ABSTRACT

The paper examines various features of the premultiplied spectra, the premultiplied derivatives of the second-order structure function (PMDS2) and three scalar parameters that characterize the anisotropic or isotropic state of the various length-scale sub-ranges within the spectra for channel flow at $Re_\tau = 4200$, generated by Lozano-Duran and Jimenez [J. Fluid Mech. 759, 432 (2014)], with the objective of inferring structural properties in the log-layer across the wave-length or eddy-size spectrum. Attention is primarily focused on the intermediate layer (“meso-layer”) covering the logarithmic velocity region within the range of wall-normal distance, y^+ , of 100–2000. Specifically, the question is addressed of whether the validity of the Attached-Eddy Hypothesis (AEH) in the log-layer can be demonstrated. It is argued that the Hypothesis needs to be reinterpreted, based primarily on the existence of a plateau region in the PMDS2, which then supports a qualified validity of the AEH right down the lower limit of the logarithmic velocity range.

INTRODUCTION

The structure of near-wall layers has been the subject of much research over many years, with conceptual descriptions of the Attached Eddy Hypothesis (AEH, henceforth) by Townsend (1980) and Perry & Chong (1982) being important historical landmarks. The fact that major efforts on canonical near-wall layers have continued unabated over the past two to three decades reflects the exceptional structural complexity of these layers awaiting full insight, as well the emergence as new opportunities to investigate open questions as a consequence of outstandingly high-quality experimental and DNS data becoming available over the past decade (Marusic *et al.* (2013); Smits *et al.* (2011); Hultmark *et al.* (2013); Rosenberg *et al.* (2013); Jiménez & Hoyas (2008); Lee & Moser (2015)). In particular, the availability of massive amounts of spatially and temporally fully-resolved raw DNS data for fairly high Reynolds numbers has opened new routes to investigating many statistical and structural properties of near-wall layers, with the objective of unravelling a variety of scale-interaction processes.

One subject of particular interest and attention has been the origin and significance of energetic large-scale structures present in the intermediate-to-outer parts of the log layer, which are the cause of a plateau, and – at sufficiently high Reynolds number – an outer (second) maximum, in the streamwise energy in the boundary layer. This behaviour is illustrated by the profiles in Fig. 1, derived from channel-flow DNS data reported by Lozano-Durán & Jiménez (2014a) and Lee & Moser (2015), respectively.

Among many processes associated with the outer structures, “footprinting” and “modulation” of small(er)-scale near-wall structures by outer structures, and implications arising from both processes to the universality of near-wall turbulence, have been major focal points of recent studies, undertaken by exploiting experimental as well as DNS data (Mathis *et al.* (2011); Ganapathisubramani *et al.* (2012); Agostini & Leschziner (2016); Agostini *et al.* (2016);

Zhang & Chernyshenko (2016)).

A question that is posed by the Reynolds-number-dependent elevation and distortion of the streamwise energy in the log-layer, depicted in Fig. 1, is whether the validity of the AEH in this layer can be defended, in view of the fact that the Hypothesis is associated with a logarithmic decline of the streamwise energy away from the wall. Townsend’s and Perry’s original interpretation was that the AEH applies to the entire velocity log-law region. Studies consistent with this view are those of Davidson *et al.* (2006a,b) and Hwang (2015). The former discusses the logarithmic behaviour of the structure function within the range $100 < y^+ < 200$, in view of the $\phi_{uu}(k_x) \propto k_x^{-1}$ behaviour that is observed by Nickels *et al.* (2005) to apply in the boundary layer at $Re_\theta = 37500$ over a similar y^+ range. Analyzing the implications of a sequence of minimal-channel simulations, each used to isolate the characteristics of a narrow size ranges of eddies, Hwang (2015) argues that the entire log-law layer is populated, as suggested by Jiménez & Hoyas (2008) and Marusic *et al.* (2013), by a hierarchical set of self-similar and self-sustaining attached eddies, in line with the original AEH. However, the above interpretation appears at odds with results derived from experimental data for high-Reynolds-number pipe flow (Hultmark *et al.* (2013), Rosenberg *et al.* (2013)) and also DNS data for channel flow at $Re_\tau = 4200$ (Lozano-Durán & Jiménez (2014a,b)), which show that the logarithmic variation of $\overline{u'u'^+}$, consistent with the k_x^{-1} behaviour, does not apply across the intermediate portion of the velocity log-law layer – referred to as the “meso-layer” henceforth – which separates the layer below $y^+ \approx 100$ from the outer region lying beyond $y \approx 0.5\delta$ (around $y^+ = 2000$ in the channel flow considered herein). Rather, a logarithmic decay of $\overline{u'u'^+}$ is observed in the remote outer region of boundary layers at very high Reynolds numbers (Hultmark *et al.* (2013); Rosenberg *et al.* (2013); Vassilicos *et al.* (2015); Vallikivi *et al.* (2015)), but this region is well beyond the log-layer and populated by “very large-scale structures”. In this outer region, the spectrum of the streamwise energy is also observed to follow $\phi_{uu}(k_x) \propto k_x^{-1}$, which is, as noted, compatible with the logarithmic decay of $\overline{u'u'^+}$.

It is against the above background and controversy that the present study set out to examine closely the structural and spectral properties of a channel-flow boundary layer at $Re_\tau = 4200$, for which extensive DNS data were generated by Lozano-Durán & Jiménez (2014a). The primary focus of the study is on an examination of the statistical properties of sub-ranges of scales within the pre-multiplied wall-normal spectra, and on a related analysis of the pre-multiplied derivative of the second-order structure function, the latter leading to a proposed alternative interpretation of the conventional AEH in the intermediate layer $100 < y^+ < 2000$.

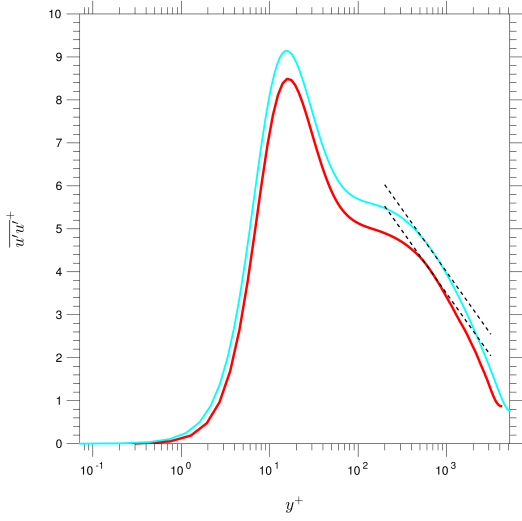


Figure 1. Wall-normal distribution of the streamwise stress at : $Re_\tau = 4200$ (red line) and $Re_\tau = 5200$ (Lee & Moser (2015)). The dashed lines represents the variation $\overline{u'u'}^+ = -1.26 \log y^+ + B$, with $B = 12.2$ and 12.7 for $Re_\tau = 4200$ and $Re_\tau = 5200$, respectively.

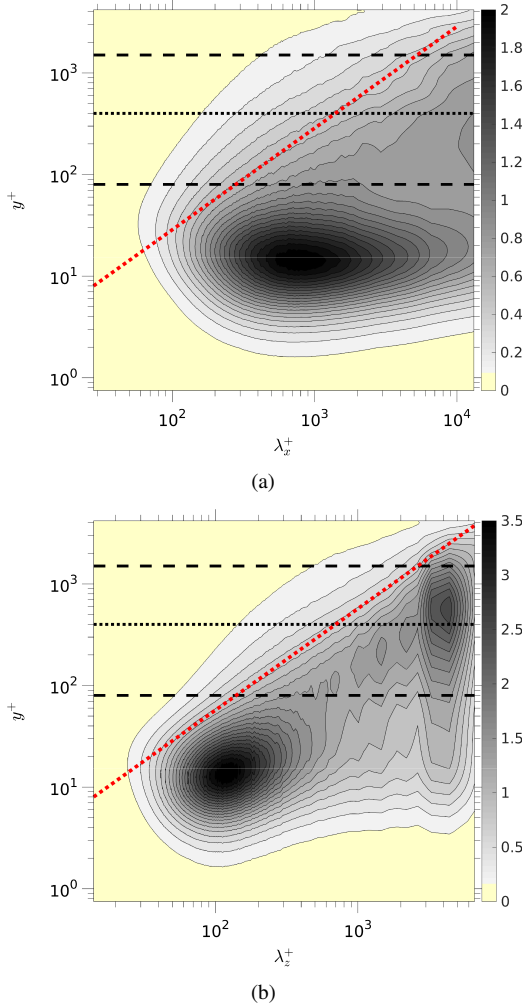


Figure 2. Pre-multiplied power spectrum of the streamwise fluctuations, in both streamwise (a) and spanwise direction (b); at $Re_\tau = 4200$. The dotted red lines show either the relation $\lambda_x^+ = 3.5y^+$ or $\lambda_z^+ = 7y^+ = 2\lambda_x^+$.

STATISTICAL PROPERTIES OF EDDY-LENGTH-SCALE SUBRANGES

Fig. 2 shows pre-multiplied spectra $k_x \Phi_{uu}(\lambda_x)$ and $k_z \Phi_{uu}(\lambda_z)$, where λ_x and λ_z are the wave numbers in the streamwise and spanwise directions, respectively. The horizontal dashed lines identify the meso-layer, on which attention focuses. Although there is an indication that the λ_x and λ_z locations at which the energy begins to rise steeply vary linearly with y^+ , in consonance with the AEH, neither spectral map features a well-defined constant-value plateau within the meso-layer. However, the existence of such a plateau, implying the variation $\Phi_{uu}(k_x) \propto k_x^{-1}$ or $\Phi_{uu}(k_z) \propto k_z^{-1}$ within a triangular region that is bounded by $\lambda_{x,min}^+ = Cy^+$ and $\lambda_{x,max}^+ = cst$ (and corresponding variations in the z^- spectra), can easily be shown to be necessary in order to satisfy the AEH-compatible logarithmic decay of the streamwise energy, such as indicated in the outer region of the meso-layer in Fig.1.

In order to shed light on the characteristics of scale subranges, some specific manipulations of the spectral maps are proposed herein. Attention focuses first of regions of isotropy of scales. Figure 3 shows two ways of highlighting such regions. The first entails the use of compensated spectra $\epsilon^{-2/3} k_x^{5/3} \Phi_{uu}$ and $\epsilon^{-2/3} k_z^{5/3} \Phi_{uu}$, which are shown in figures 3(a) and 3(b), respectively, where ϵ is a surrogate of rate of turbulence-energy dissipation, defined such as $\epsilon = \overline{\omega_k \omega_k} / 3$. The red lines in the x -wise and z -wise maps are defined, respectively, by $\lambda_x^+ = 3.5 \times y^+$ and $\lambda_z^+ = 7 \times y^+ = 2 \times \lambda_x^+$, while the blue lines describe, respectively, the variations $\lambda_x^+ = 3.5 \times (y^+)^{1/3}$ and $\lambda_z^+ = 7 \times (y^+)^{1/3} = 2 \times \lambda_x^+$. The red and blue lines bound, approximately, plateau regions characteristic of near-isotropy. The second route rests on the definition of the following ‘‘isotropy parameter’’:

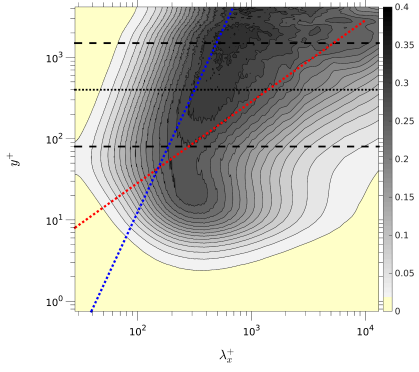
$$\gamma^{3c} \equiv \frac{3|\Phi_{uu}||\Phi_{vv}||\Phi_{ww}|}{|\Phi_{uu}|^3 + |\Phi_{vv}|^3 + |\Phi_{ww}|^3} \quad (1)$$

in which Φ_{uu} , Φ_{vv} and Φ_{ww} are the x -wise or z -wise spectra for the three components u , v and w , respectively. This parameter tends to a maximum of 1 in the case of isotropy, declining to zero in the case of a two-component or a one-component state. The maps in figures 3(c) and 3(d) show (for greater visual impact) the square of γ^{3c} as functions of λ_x^+ and λ_z^+ , respectively. The fact these regions of high γ^{3c} are, again, bounded by the red and blue lines and broadly coincide with the near-plateau regions in the compensated spectra supports the proposition that these regions within the meso-layer characterize detached eddies.

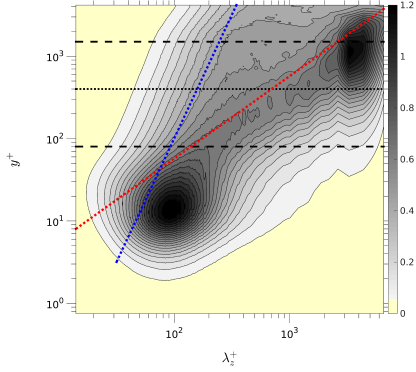
An analogous route to that taken above is adopted next to delineate regions of elevated anisotropy. Thus, a parameter that identifies the dominance of the streamwise component over the two others is:

$$\gamma_u^{1c} \equiv \frac{|\Phi_{uu}|^2}{|\Phi_{uu}|^2 + |\Phi_{vv}|^2 + |\Phi_{ww}|^2} \quad (2)$$

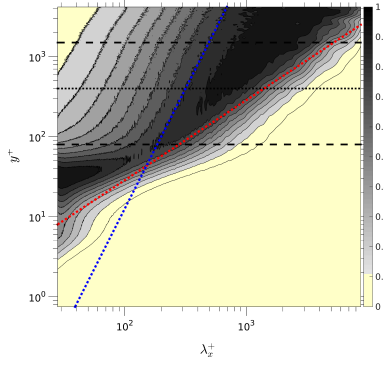
This parameter tends to 1 when the energy is increasingly contained in the Φ_{uu} spectra, and diminishes when the anisotropic state departs from the one-component condition. Maps of $(\gamma_u^{1c})^3$ in the x and z directions (the cubic exponent designed to accentuate gradients in the maps) are shown in figures 4(a) and 4(b), respectively. Both maps reveal that, within the meso-layer, the dominance of the streamwise component is confined to the larger scales beyond the boundaries identified by the red lines, and this is the attached-eddy region, as will be argued in the following Section. In fact, the most pronounced regions in figure 4 pertain to scales which are the subject of many studies that deal with elongated large-scale structures



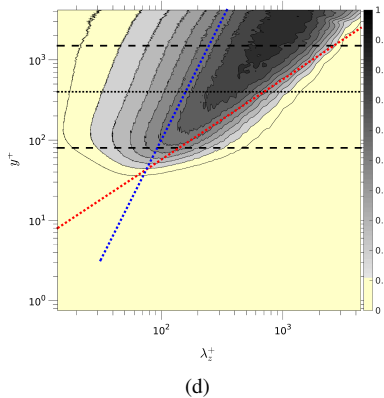
(a)



(b)

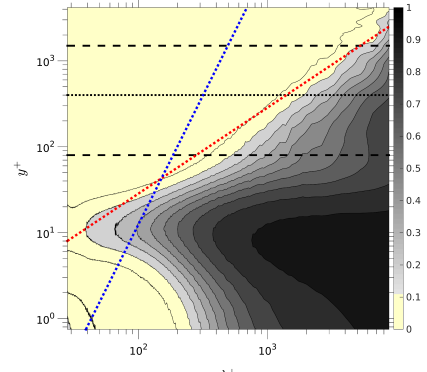


(c)

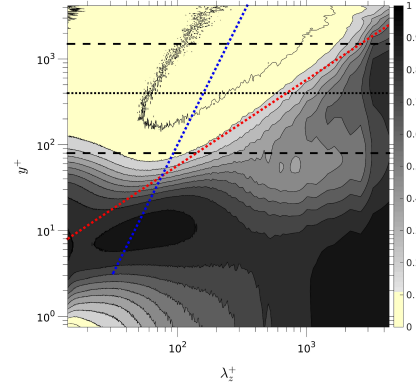


(d)

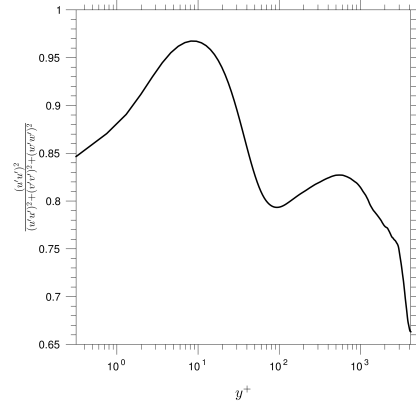
Figure 3. Characterisation of isotropy across eddy-size range: (a) compensated spectra $\varepsilon^{-2/3} k_x^{5/3} \Phi_{uu}$, (b) compensated spectra $\varepsilon^{-2/3} k_z^{5/3} \Phi_{uu}$, (c) and (d) maps of the square of the “isotropy parameter” $(\gamma^{3c})^2$, derived from the streamwise and spanwise spectral components. The red lines show either the relation $\lambda_x^+ = 3.5y^+$ or $\lambda_z^+ = 7y^+ = 2\lambda_x^+$ and the blue lines show either the relation $\lambda_x^+ = 3.5(y^+)^{1/3}$ or $\lambda_z^+ = 7(y^+)^{1/3} = 2\lambda_x^+$.



(a)



(b)



(c)

Figure 4. Characterisation of anisotropy due to dominance of streamwise energy $\overline{u'u'^+} \gg \overline{v'v'^+}, \overline{w'w'^+}$: (a) maps of $(\gamma_u^{1c})^3$ in streamwise direction, (b) maps of $(\gamma_u^{1c})^3$ in spanwise direction and (c) cross-spectrum average of γ_u^{1c} . Red and blue dotted lines: see caption of figure 3.

in the outer part of the log-layer (Marusic (2001)). Figure 4 also contains a y^+ -wise profile of the normalised streamwise energy, and this provides confirmation of the existence of energetic structures in the outer layer around $y^+ \approx 500$. Reference to the $(\gamma_u^{1c})^3$ distribution along the dotted black line at $y^+ = 500$ clearly shows that this peak in streamwise energy is associated with structures having wavelengths of order $\lambda_x^+ \gtrsim 8000$ and $\lambda_z^+ \gtrsim 4000$. The near-wall energy peak, at $y^+ \approx 10$ is also clearly brought out in the $(\gamma_u^{1c})^3$ maps, in which a maximum at $\lambda_z^+ \approx 100$ is evidently indicative of the strong small-scale streaks in the buffer layer.

The maps shown in figures 3 and 4 contain small-scale ranges

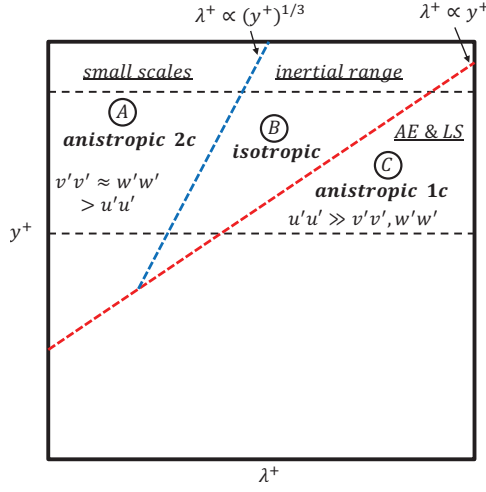


Figure 5. Sub-ranges in spectral map having distinct turbulence characteristics (1c: dominance of streamwise component; 2c: dominance of cross-flow components).

to the left of the blue lines $\lambda^+ \propto (y^+)^{\frac{1}{3}}$ which neither comply with isotropy nor with one-component dominance. The scales in question are not far from the Kolmogorov range $\lambda^+ \propto (y^+)^{\frac{1}{4}}$. The properties of these ranges have also been investigated, for example, by way of a third anisotropy parameter, γ_{ij}^{2c} , defined as:

$$\gamma_{ij}^{2c} \equiv \frac{2|\Phi_{ii}||\Phi_{jj}|}{|\Phi_{uu}|^2 + |\Phi_{vv}|^2 + |\Phi_{ww}|^2} \quad (3)$$

identifying the dominance of two normal components, $i \neq j$, over the third, and thus highlights the range where the anisotropic turbulence is characteristic of two-component turbulence. The results of this part of the study are not central to the key arguments and conclusions presented below, and they will therefore be reported in a more comprehensive paper to follow.

The eddy-scale sub-regions identified on the basis of the above analysis are shown in Fig.5. Of primary relevance and interest is sub-region C, characterized by a dominance of the streamwise energy component, relative to the two others, in the region in which the length scales of the structures is relatively large. Eddies having smaller length scales, located within region B, are close to isotropic, in terms of energy, do not carry shear stress and are therefore deemed “detached”. In contrast, the state in region C is characterized by anisotropy, with streamwise energy dominating, and the eddies are affected by shear, carry shear stress and thus comply with the notion of “attached” eddies.

THE ATTACHED EDDY HYPOTHESIS

In the absence of a clear region of $\Phi_{uu} \propto k^{-1}$, conventionally associated with the Townsend-Perry AEH, attention is directed to an investigation of maps of the pre-multiplied derivatives of the second-order structure function (“PMDS2”, henceforth) $\delta \times \frac{dS_{2,u}(\delta)}{d\delta}$, where δ is the separation. The structure-function analysis is performed over both directions, x and z separately; in the streamwise direction, $S_{2,u}(y, \delta)$ is defined as $\left\langle [u(y, x) - u(y, x + \delta)]^2 \right\rangle_{z,t}$, the subscripts z, t identifying homogeneous averaging directions. Such maps are shown in Fig. 8. The rationale of focusing on these maps arises from the observation by Davidson *et al.* (2006a,b) that there is a close relationship between $S_{2,u}$ and the pre-multiplied

spectra. However, the advantage of the PMDS2 is that plateau regions in these map are more pronounced and thus more readily identifiable as being associated with the AEH than in the corresponding spectral maps.

The PMDS2 expresses the contribution to the energy associated with eddies having a length δ . This is equivalent to, but not the same as, the pre-multiplied power spectra ($k\Phi_{uu}$). Given a constant level of the PMDS2, which is consistent with a k^{-1} variation of the spectrum (Davidson *et al.*), integration then immediately yields a logarithmic variation of $S_{2,u}(\delta/y)$ and thus a logarithmic dependence $\overline{u'u'}^+(\delta/y)$ for $\delta = L$. There is, therefore, a mutually consistent linkage between a k^{-1} spectrum, a constant level of the PMDS2, the logarithmic variation of $\overline{u'u'}^+$ and the AEH. It is not surprising, therefore, to observe a striking similarity between the pre-multiplied power spectra and the corresponding PMDS2, as emerges upon comparing the maps in figures 7(a) and (b) with those in figure 2. The relevant test in respect of the AEH is thus whether $\delta dS_{2,u}/d\delta = cst$.

In the previous Section, it was proposed that the meso-layer may be divided into three physically different domains - A, B and C (figure 5). These are associated, respectively, with spectra of the form $\phi_{uu} \sim \epsilon^{1/3} k_x^{-7/3}$, $\phi_{uu} \sim \epsilon^{2/3} k_x^{-5/3}$ and $\phi_{uu} \sim k_x^{-1}$, the last indicative of the AEH. As argued by Pope (2001), a power-law spectrum $\Phi(\omega) \approx C_1 \omega^{-p}$ can be related to the second-order structure function $S_p(\delta) \approx C_2 \delta^q$ with $p = q + 1$, valid only under the condition that $p > 1$. In accordance with the AEH, $p = 1$, in which case Davidson *et al.* (2006a,b) show that $S^2(\delta) \approx C_3 \log(\delta) + B$. The implications for subregions A, B and C in figure 5 are therefore, respectively:

$$\begin{aligned} \text{region A: } & \delta_x dS_{2,u}/d\delta_x \sim \epsilon^{1/3} \delta_x^4 \\ \text{region B: } & \delta_x dS_{2,u}/d\delta_x \sim \epsilon^{2/3} \delta_x^2 \\ \text{region C: } & \delta_x dS_{2,u}/d\delta_x = cst \end{aligned}$$

Figure 6(a) shows a map of $\delta_x \frac{dS_{2,u}}{d\delta_x}$ compensated by $\epsilon^{-1/3} \delta_x^{-4/3}$. As expected, on the basis of the above statements on the spectra, there is a “plateau” in region A, bounded by the blue line. Figure 6(b) relates to the isotropic state through the augmentation by $\epsilon^{-2/3} \delta_x^{-2/3}$, along with a normalized version thereof in figure 6(c), in which the levels at any y -value are normalised by the maximum at that level. Both maps bring to light the plateau in region B in the meso-layer, bounded by the blue and red lines. This region is narrow in the lower part of the layer, but broadens as y increases – i.e. the inertial range becomes wider in the outer portion of the log-layer. These features concur with those in the map in figure 4 showing the parameter $(\gamma^{2c})^2$ (see equation 1). The PMDS2 maps shown in figure 7(a) and (b) – especially the latter – include an oblique band to the right of, and parallel to, the red line, i.e. region C, in which the condition $\delta_x dS_{2,u}/d\delta_x = cst$ is met, at least approximately. Although this provides some support for the validity of the AEH in the meso-layer, the absence of a well-defined plateau is counter-indicative.

Evidence in support of the AEH is provided by features contained in the maps of the PMDS2, figures 7(a) and (b), in which two regions are highlighted: a blue triangular region and a more restricted red trapezoidal region, both covering the meso-layer. If a perfect plateau in the PMDS2 and the corresponding pre-multiplied spectra existed within the triangular region, the implications regarding the AEH would be those shown in schematic 8(a). In this conceptual schematic, a sequence of four attached eddies, $e_1 - e_4$, are given, whose energy rises with height such that the eddies collapse if the energy density and height are normalised by $\lambda = 1/k = y$ i.e., the eddies are self-similar. If these eddies exist in the triangular re-

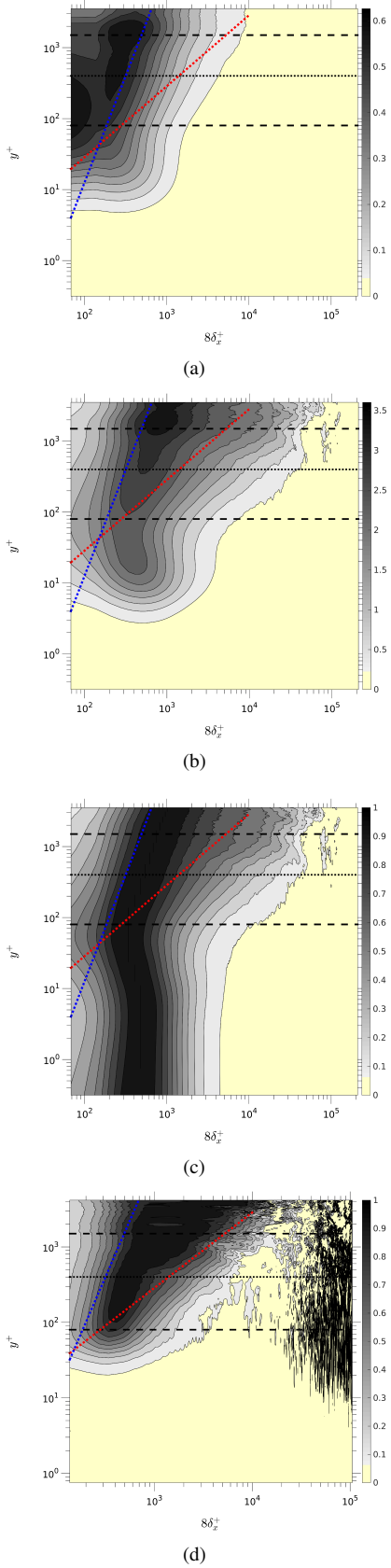


Figure 6. Turbulence state, premultiplied derivative of the structure function compensated by : (a) $\varepsilon^{-1/3}\delta_x^{-4/3}$, (b) $\varepsilon^{-2/3}\delta_x^{-2/3}$; (c) the compensated $\delta_x \frac{dS_{2u}}{d\delta_x}$ defined for the isotropic case is divided by the maximum value at each y -location and (d) isotropic parameter $(\gamma^{3c})^2$. Red and blue dotted lines: see caption of figure 3.

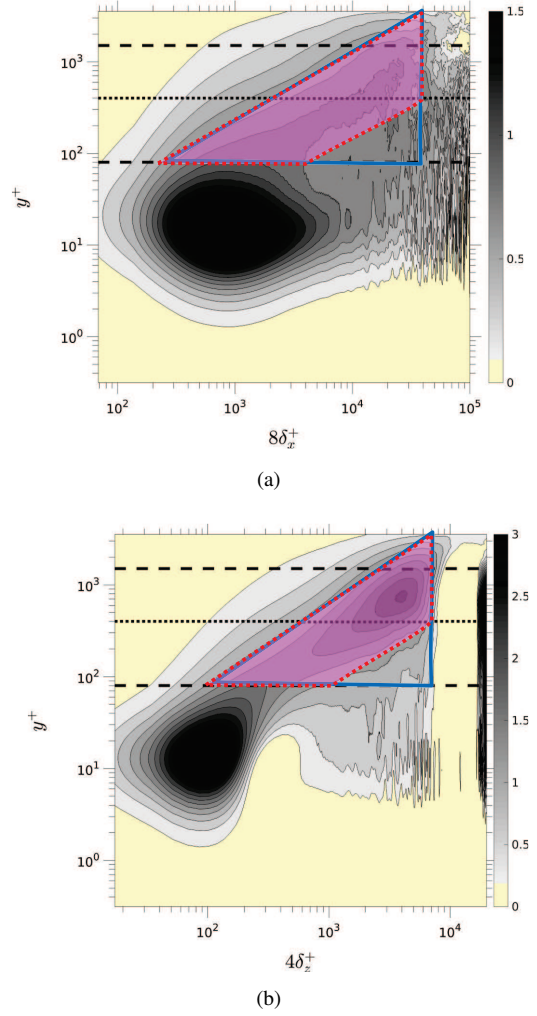


Figure 7. Maps of PMDS2 with δ taken in streamwise (a) and spanwise (b) direction, respectively.

gion of the spectrum, within which $k\Phi_{uu} = cst = A$, limited between $\lambda_{min} = y$ and $\lambda_{max} = cst$, it follows that the energy $\overline{u'u'}$ varies logarithmically with y . The implication is thus that, at any y -location, only eddies larger than the attached eddy at that height contribute to the energy, and that all such eddies contribute at the level $k\Phi_{uu} = A$.

As is evident from figure 7(a) and (b), there is no clear plateau within the triangular region. However, there is an approximately constant level within the red trapezoidal region. One consequence of this restricted plateau region is that the logarithmic variation of $\overline{u'u'}$ only applies in the upper portion of the meso-layer, above the dotted line in figures 7(a) and (b). Below that line, the linear variation of the parallel boundaries of the trapezoid, when transcribed to the pre-multiplied spectra, implies a constant level of $\overline{u'u'}$, broadly in line with the variations shown in figure 1.

Figure 8(b) now pertain to the trapezoidal domain shown in figures 7(a) and (b). The upper part of this domain is triangular, which thus conforms to the relationship shown in figure 8(a). Figures 8(b) relate to the parallelogram below the triangular region. As before, the normalisation $k\Phi_{uu} = A$ applies, but only over a restricted height of the eddies. Below the height defined by the lower line of the parallelogram $\lambda_{max}(y)$, the energy of the eddy declines rapidly. If, next, $\overline{u'u'}$ is evaluated by integration between the parallel lines $\lambda_{min}(y)$ and $\lambda_{max}(y)$ – the lines bounding the parallelogram – the result is a plateau of $\overline{u'u'}$.

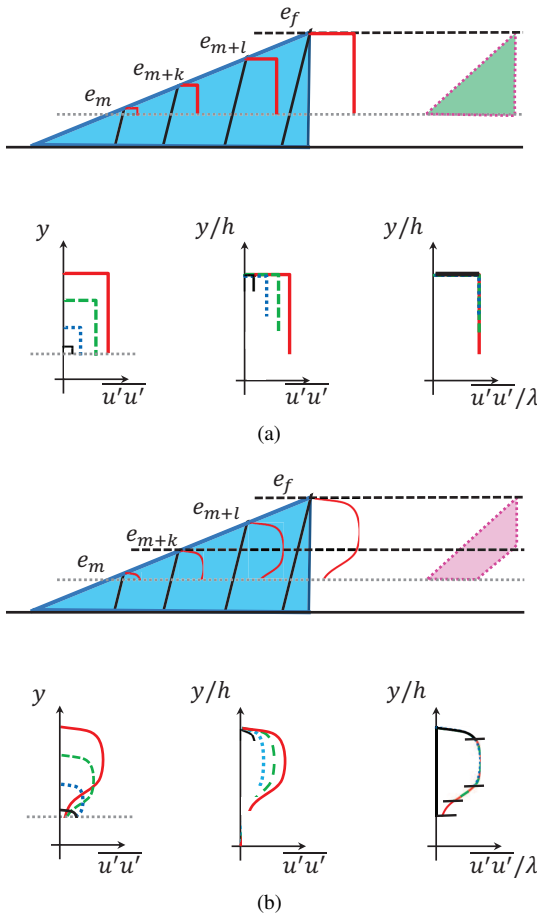


Figure 8. Conceptual representation of AE self-similarity through the meso-layer : velocity profile associated to (a) the original AEH and (b) augmented AEH.

This representation differs substantially from the conventional AEH, but does imply a self-similar set when scaling with h and λ is effected. It is thus arguable that the plateau region within the trapezoidal region in figures 7(a) and (b) is fundamentally consistent with the AEH even though there is no clearly defined triangular plateau region. This interpretation also explains, at least in principle, the plateau in the $\overline{u'u'}$ profile, by virtue of the fact that integration of the premultiplied spectra across the λ range within the lower portion of the trapezoidal section yields a constant level of $\overline{u'u'}$.

CONCLUSIONS

The examination of the streamwise and spanwise structure functions has revealed the existence of a trapezoidal (rather than triangular) region of nearly constant value spanning the entire meso-layer, $100 < y^+ < 2000$, not observed in the associated premultiplied spectra. This led to the proposition of an augmented form of the Attached Eddy Hypothesis covering the meso-layer, thus accommodating the plateau region in the streamwise- energy profile, with its centre being at $y^+ \approx 300$.

REFERENCES

Agostini, Lionel & Leschziner, Michael 2016 On the validity of the quasi-steady-turbulence hypothesis in representing the effects of large scales on small scales in boundary layers. *Physics of Fluids (1994-present)* **28** (4), 045102.

- Agostini, L., Leschziner, M. & Gaitonde, D. 2016 Skewness-induced asymmetric modulation of small-scale turbulence by large-scale structures. *Physics of Fluids* **28** (1), 015110.
- Davidson, PA, Krogstad, P-A, Nickels, TB *et al.* 2006a A refined interpretation of the logarithmic structure function law in wall layer turbulence. *Physics of Fluids* **18** (6), 5112.
- Davidson, PA, Nickels, TB & Krogstad, P- 2006b The logarithmic structure function law in wall-layer turbulence. *Journal of Fluid Mechanics* **550**, 5160.
- Ganapathisubramani, B, Hutchins, N, Monty, JP, Chung, D & Marusic, I 2012 Amplitude and frequency modulation in wall turbulence. *Journal of Fluid Mechanics* **712**, 6191.
- Hultmark, Marcus, Vallikivi, M, Bailey, SCC & Smits, AJ 2013 Logarithmic scaling of turbulence in smooth-and rough-wall pipe flow. *Journal of Fluid Mechanics* **728**, 376395.
- Hwang, Y. 2015 Statistical structure of self-sustaining attached eddies in turbulent channel flow. *Journal of Fluid Mechanics* **767**, 254289.
- Jiménez, J. & Hoyas, S. 2008 Turbulent fluctuations above the buffer layer of wall-bounded flows. *Journal of Fluid Mechanics* **611**, 215236.
- Lee, M. & Moser, R. D. 2015 Direct numerical simulation of turbulent channel flow up to $Re\tau \approx 5200$. *Journal of Fluid Mechanics* **774**, 395415.
- Lozano-Durán, A. & Jiménez, J. 2014a Effect of the computational domain on direct simulations of turbulent channels up to $Re\tau = 4200$. *Physics of Fluids* **26** (1), 011702.
- Lozano-Durán, A. & Jiménez, J. 2014b Time-resolved evolution of coherent structures in turbulent channels: characterization of eddies and cascades. *Journal of Fluid Mechanics* **759**, 432471.
- Marusic, I. 2001 On the role of large-scale structures in wall turbulence. *Physics of fluids* **13**, 735.
- Marusic, Ivan, Monty, Jason P, Hultmark, Marcus & Smits, Alexander J 2013 On the logarithmic region in wall turbulence. *Journal of Fluid Mechanics* **716**, R3.
- Mathis, R., Hutchins, N. & Marusic, I. 2011 A predictive inner-outer model for streamwise turbulence statistics in wall-bounded flows. *Journal of Fluid Mechanics* **681**, 537566.
- Nickels, TB, Marusic, I, Hafez, S & Chong, MS 2005 Evidence of the k^{-1} law in a high-Reynolds-number turbulent boundary layer. *Physical review letters* **95** (7), 074501.
- Perry, AE & Chong, MS 1982 On the mechanism of wall turbulence. *Journal of Fluid Mechanics* **119**, 173217.
- Pope, Stephen B 2001 Turbulent flows.
- Rosenberg, BJ, Hultmark, Marcus, Vallikivi, M, Bailey, SCC & Smits, AJ 2013 Turbulence spectra in smooth-and rough-wall pipe flow at extreme Reynolds numbers. *Journal of Fluid Mechanics* **731**, 4663.
- Smits, Alexander J, McKeon, Beverley J & Marusic, Ivan 2011 High-Reynolds number wall turbulence. *Annual Review of Fluid Mechanics* **43**, 353375.
- Townsend, Albert A 1980 *The structure of turbulent shear flow*. Cambridge university press.
- Vallikivi, M., Ganapathisubramani, B. & Smits, AJ 2015 Spectral scaling in boundary layers and pipes at very high Reynolds numbers. *Journal of Fluid Mechanics* **771**, 303.
- Vassilicos, JC, Laval, J-P, Foucaut, J-M & Stanislas, Michel 2015 The streamwise turbulence intensity in the intermediate layer of turbulent pipe flow. *Journal of Fluid Mechanics* **774**, 324341.
- Zhang, Chi & Chernyshenko, Sergei I 2016 Quasisteady quasihomogeneous description of the scale interactions in near-wall turbulence. *Physical Review Fluids* **1** (1), 014401.